Revue de primatologie

Numéro 2 (2010)
Varia

Nelly Joseph-Mathurin, Olene Dorieux, Audrey Kraska, Anne Bertrand, Mathieu Santin, Nadine El Tannir El Tayara et Marc Dhenain

Magnetic resonance imaging in primates. The example of the mouse lemur (*Microcebus murinus*): From detection of pathological aging to therapeutic evaluations

Référence électronique
Nelly Joseph-Mathurin, Olene Dorieux, Audrey Kraska, Anne Bertrand, Mathieu Santin, Nadine El Tannir El Tayara et Marc Dhenain, « Magnetic resonance imaging in primates. The example of the mouse lemur (*Microcebus murinus*): From detection of pathological aging to therapeutic evaluations », *Revue de primatologie* [En ligne], 2 | 2010, document 5, mis en ligne le 15 juin 2011. URL : http://primatologie.revues.org/508
DOI : en cours d'attribution

Éditeur : Société francophone de primatologie
http://primatologie.revues.org
http://www.revues.org

Document accessible en ligne sur :
http://primatologie.revues.org/508
Document généré automatiquement le 15 décembre 2010.

Nelly Joseph-Mathurin, Olene Dorieux, Audrey Kraska, Anne Bertrand, Mathieu Santin, Nadine El Tannir El Tayara et Marc Dhenain

Magnetic resonance imaging in primates. The example of the mouse lemur (*Microcebus murinus*): From detection of pathological aging to therapeutic evaluations

Historique
Soumis juillet 2010. Accepté décembre 2010

1 Introduction

1 Cerebral aging is a major public health issue in our societies as the aged population is dramatically increasing. It leads to cognitive alterations called "Age Associated Memory Impairment" (AAMI) in 1/3 of the non-demented aged persons (Crook *et al.*, 1986). The origin of these alterations is still widely unknown. In many cases, cerebral aging leads to more severe alterations and is associated to neurodegenerative diseases and dementia. The most common neurodegenerative disease is Alzheimer's disease (AD). It represents 60 to 70% of all dementia cases. The second cause of dementia is vascular dementia (stroke and multi-infarct lesions) which represents 15 to 20% of dementia cases (Fratiglioni *et al.*, 2000). Parkinson's disease (PD) is the third cause of neurological disease in aged humans (Rocca, 2000). Understanding the physiopathology of cerebral aging and associated neurodegenerative diseases requires the use of animal models. Such models are also critical to evaluate the efficiency of new drugs. Old rodents, rodents that underwent surgery or intoxication by drug treatments, and transgenic mice are widely used as models of cerebral aging (Shimada *et al.*, 1992), Alzheimer's disease (Delatour *et al.*, 2006b), stroke (Carmichael, 2005) or Parkinson’s disease (Harvey *et al.*, 2008). However, because of the phylogenetic distance with humans, they do not recapitulate the full range of clinical symptoms and microscopical lesions presented by humans, and they are often poorly predictive of the efficiency of drugs in humans.

2 Non-human primates are thus used as complementary models. For example macaques treated with MPTP toxin or that received dedicated surgeries are used as models of Parkinson's disease (Jarraya *et al.*, 2009) or stroke (Fukuda et del Zoppo, 2003). Macaques are also widely used for research on cerebral aging and age-associated neurodegenerative diseases such as Alzheimer's disease (Price *et al.*, 1991; Uno *et al.*, 1996; Roth *et al.*, 2004; Lacreuse et Herndon, 2009). Indeed macaques can develop with aging alterations characteristic of AD such as extracellular amyloidosis (Uno *et al.*, 1996) and tauopathy (Oikawa *et al.*, 2010). Moreover, they present age-associated cognitive alterations (Bartus et Dean, 1985) that can be linked to neuronal atrophy or loss (Smith *et al.*, 2004). Using large primates as models of cerebral aging is however associated to some difficulties because of their large size and long maximum life span (30 years for the Rhesus monkeys (Tigges *et al.*, 1988)).

3 An alternative model is the mouse lemur primate (*Microcebus murinus*). It is a small animal that can be used as a model of cerebral aging (Aujard *et al.*, 2001) or Alzheimer's disease (Mestre-Frances *et al.*, 2000). As compared to large primates, mouse lemurs present many advantages. They have a small size (about 12 cm, 100 g) and have a mean life span of 5 years and a maximum life span of 12 years in captivity (Perret, 1997). Their brain weighs approximately 1.7 g (Bons *et al.*, 1998). It measures 23 mm from the tip of the olfactory bulbs

to the caudal end of the medulla, and has a maximum width of 18 mm (Le Gros Clark, 1931). Previous studies have shown that some aged mouse lemurs can present some of the lesions that characterize AD such as extracellular amyloid deposits (Bons *et al.*, 1991) or altered tau proteins (Bons *et al.*, 1995; Delacourte *et al.*, 1995). Some aged animals also display cognitive alterations that are correlated to cerebral atrophy (Picq *et al.*, 2010).

4 Studying nonhuman primate models of human diseases can be difficult due to animal heterogeneity and also because of the small number of available animals. Moreover, for ethical reasons, sacrificing aged primates has to be limited. Non invasive methods that allow for neurological follow-up of aged primates are thus useful to evaluate cerebral anatomy, cerebral aging and associated neuropathological changes, as well as therapeutic interventions. For example several magnetic resonance imaging (MRI) methods have been used in macaques to highlight brain changes during the aging process (Andersen *et al.*, 1999; Lacreuse *et al.*, 2005; Makris *et al.*, 2010; Koo *et al.*, 2010). MRI can also be used in more convenient models such as mouse lemur primates to better understand brain aging. In this article, we will focus on the characterization of mouse lemur primate brain in normal conditions and during normal and pathological aging, using MRI.

5 First, the principle of MRI will be presented. Then, results concerning the description of cerebral anatomy and brain aging by MRI in mouse lemurs will be presented. Finally, other applications of MRI will be described to ameliorate studies of brain metabolism by registering MR and positron emission tomography (PET) images, to perform cerebral surgery in mouse lemurs, and to evaluate new therapies.

2 Generalities on MRI

6 Magnetic resonance imaging is a method that has been developed in the early 70th (Lauterbur, 1973; Mansfield et Grannell, 1973) and is based on nuclear magnetic resonance technique. Its discovery was awarded the Nobel Prize in Physiology or Medicine in 2003. This method relies on strong magnetic field and radiofrequency (RF) waves to provide images of internal anatomy including brain tissues. The magnetic field strength is measured in Tesla (1 Tesla corresponds to ~20 000 times the earth magnetic field). For brain imaging in lemurs, field strengths from 4.7 to 11.7 Tesla have been used. The general principle of MRI can be overviewed as follows (Fig. 1): animal tissues contain large amount of water molecules. In these water molecules, hydrogen atom nuclei correspond to single protons displaying a magnetic moment called spin, which means that they behave as small compass (Fig. 1A). This magnetic moment can be represented as a small magnetic vector. In the presence of the strong magnetic field created by the MR scanner, the magnetic moments of the hydrogen atoms line up with the direction of the magnetic field and create a stronger vector called magnetization. In this condition, spins are at the equilibrium (Fig. 1B). They also rotate at a frequency (Larmor frequency or resonance frequency) which depends on the strength of the magnetic field. Then, RF waves created by the MR scanner at the resonance frequency are used to flip the magnetization into a transverse plan (Fig. 1C). Once flipped, the magnetization comes back to the equilibrium (the “relaxation” process) with a speed that depends on the chemical properties of surrounding tissues (Fig. 1D). Thus, different types of tissue (gray matter, white matter, cerebro-spinal fluid…) give off different types of “tissue specific” signal (corresponding to the speed of magnetization relaxation) following the application of the same RF pulse. Furthermore, additional magnetic fields called "gradients" are used to slightly modify the strong magnetic field of the magnet, in order to select the spins that will flip during the emission of the radiofrequency wave. This process allows for the localization of the MR signal. Finally, the decrease of MR signal, linked to the speed of magnetization relaxation, can be detected by the MR scanner and is transformed into an image thanks to signal processing algorithms (Fourier transform). The parameters that command the contrast in MR images are called relaxation times. One can differentiate the

longitudinal relaxation time (T1) and the transverse relaxation times (T2 and T2* (T2 star)). These parameters are dependent on the composition of tissues. Images that rely on T1, T2, or T2* contrasts are called T1-weighted (T1-w), T2-weighted (T2-w) and T2*-weighted (T2*-w) images.

Figure 1

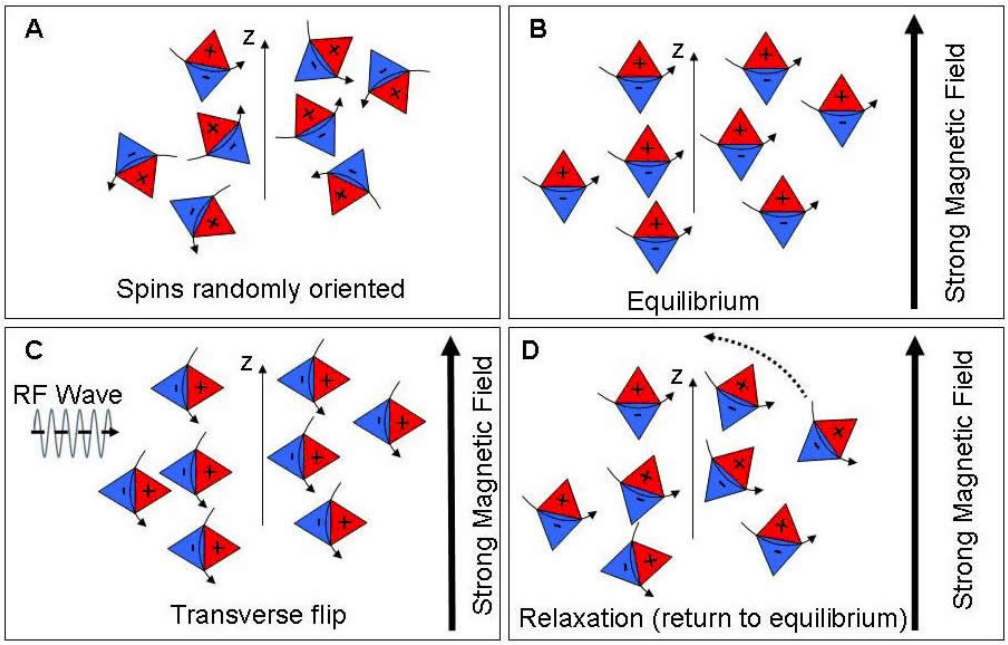

Basic principle of MRI. A. Spins randomly oriented. B. Spins oriented in the direction of the strong magnetic field of the MRI. C. Radiofrequency wave flips the spins on a transverse plan. D. The spins that are in this position created an MRI signal. The return to the equilibrium (relaxation) of the spins occurs with different speeds when the spins are located in different tissues. Speed difference of relaxation between spins provides contrast between the different tissues.
Principe de base de l'IRM. A. Spins orientés aléatoirement. B. Spins orientés dans la direction du champ magnétique fort de l'IRM. C. L'onde radiofréquence bascule les spins dans le plan transversal. D. Les spins dans cette position créent un signal IRM. Le retour à l'équilibre (relaxation) des spins s'effectue à différentes vitesses en fonction des tissus environnants. La différence de vitesse de relaxation entre les spins est à l'origine du contraste entre les différents tissus.

7 Although MR was first developed in humans, it is now largely used in animals. Figure 2 shows examples of MR images recorded in mice, mouse lemurs and macaques. One can see that images of good quality can be acquired in mouse lemurs, despite the small size of these animals.

8 One of the main advantages of MRI is that it does not use ionizing forms of “x-ray” or "radioactive" energy, potentially harmful to living tissue, unlike CT-scans or positron emission tomography (PET). This built-in safety feature makes MRI an ideal non-invasive tool for the imaging of human or animals in order to better understand the physiological norms of brain anatomy and function. A second interesting aspect of MRI is that it allows for the detection of different biological parameters: for example, microscopic anatomy (Kappeler *et al.*, 2007), vascular system by MR angiography (El Tannir El Tayara *et al.*, 2010), cerebral perfusion by blood (Faure *et al.*, 2009), and brain activation (Yu *et al.*, 2010).

Figure 2

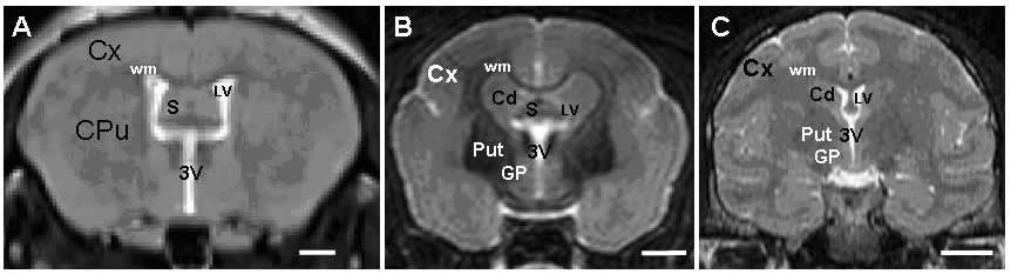

Comparison of MRI (T2-weighted sequences, coronal view at the level of caudate and putamen nuclei) in a mouse (A), a mouse lemur (B) and a macaque (C). The scale bar for mouse, mouse lemur and macaque images are 1mm, 2.5mm and 10mm respectively. Major brain structures are annotated: CPu: Caudate Putamen (=striatum in mice); Cd: Caudate; Pu: Putamen; GP: Globus pallidus; Cx: Cortex; S: Septum; wm: white matter, LV: Lateral ventricle; 3V: Third ventricle.
Comparaison d'IRM (séquences pondérées en T2, vue coronale au niveau du noyau caudé et du putamen) chez une souris (A), un microcèbe (B) et un macaque (C). Les barres d'échelle pour la souris, le microcèbe et le macaque sont respectivement 1mm, 2.5mm et 10mm. Annotations des structures principales: CPu: Noyau caudé / putamen (=striatum chez la souris); Cd: Noyau caudé; Pu: Putamen; GP: Globus pallidus; Cx: Cortex; S: Septum; wm : substance blanche, LV: Ventricule latéral; 3V: Troisième ventricule.

3 MR Imaging protocols in mouse lemurs

9 MRI spectrometers dedicated for imaging primates are sparse. However adult macaques and larger primates can be scanned with human MR spectrometer (Andersen *et al.*, 2002; Leite *et al.*, 2002) although standard human RF coils are not optimized for primate brains. The mouse lemur primate has the advantage to have a brain size between the rat and the mouse. Preclinical scanners adapted for small animals can thus be used to image their brains at high magnetic field. These scanners allow good spatial resolution to record MR images in the mouse lemur.

3.1 *In vivo* imaging protocols

10 MR exams are performed in anesthetized mouse lemurs. Anesthesia prevents animal motion during the image acquisition that lasts approximately 45 minutes. Typically, animals are pre-medicated with atropine (0.025 mg/kg subcutaneously) and anesthetized by isoflurane. Animals are then usually installed in a stereotaxic frame before to be inserted in the MR scanner. Respiration rate is monitored to insure animal stability until the end of the experiment. Body temperature of the mouse lemur is maintained at 30-33°C by using a water-filled heating blanket. Several imaging protocols can be performed depending on the parameter to be evaluated. Typical imaging parameters for *in vivo* imaging of cerebral anatomy are based on three-dimensional inversion-recovery fast spin-echo images (IR-RARE) with an isotropic nominal resolution close to 200 µm (other imaging parameters: TR/TE=2500/6 msec, TEw=45 msec, TI=200 msec, RARE-factor=16) (Dhenain *et al.*, 2003) (Fig. 2B).

3.2 *Ex vivo* imaging protocols

11 Although MRI is traditionally considered as an *in vivo* imaging method, *ex vivo* MRI can be very useful for acquiring 3D histological images of the brain. As this method does not require any sample slicing, it avoids the distortions inherent to histological processing. Our group implemented a method called Gadolinium-staining (or passive staining) (Dhenain *et al.*, 2006). It consists on soaking the fixed brains in a solution of 0.5 M gadoterate (Gadolinium) meglumine at a dilution of 1:200 (2.5 mM) in phosphate buffered saline (PBS), for at least 24 hours prior to MR imaging. The gadolinium contrast agent passively diffuses into the tissue, increasing the contrast between the different types of tissues and allowing for high-resolution imaging with still a good signal-to-noise ratio. For example, such a protocol applied in lemurs allows for the acquisition of MR images with a resolution of (31 x 31 x 120) μm^3 (Fig. 3).

4 Use of MRI to describe brain anatomy

4.1 Imaging neuroanatomy

12 *In vivo* images of mouse lemur brains highlight the morphological neuroanatomy of mouse lemurs. For example, the dissociation between the caudate and putamen, a specific feature of primates, is clearly visible on *in vivo* MR images of mouse lemur brains (compare Fig. 2B to Fig. 2A).

13 The use of passive staining protocols coupled with micro-MRI *ex vivo* acquisitions lead to a refined description of mouse lemur neuroanatomy (Fig. 3). The subregions of the hippocampal formation, i.e. the dentate gyrus (DG), the Ammon's horn (AH) and the subiculum (Sub), can be nicely differentiated (Fig. 3B). Fine white matter tracts, such as the perforating fibers of the median longitudinal fasciculus (MLF), can be detected (Fig. 3D). Individual cellular layers can be resolved; for instance in the olfactory bulb, the mitral cell layer (< 100 micron thickness) can be clearly differentiated from the internal and the external plexiform layers, which appear more hyperintense (=brighter) than the mitral cell layer (Fig. 3E). The excellent contrast-resolution between brain structures after passive staining, together with the acquisition of 3D images, allow for volumetric measurements of specific subregions of the brain. *Ex vivo* MRI can thus provides information on subtle anatomy of the brain down to the resolution of individual cell layers.

Figure 3

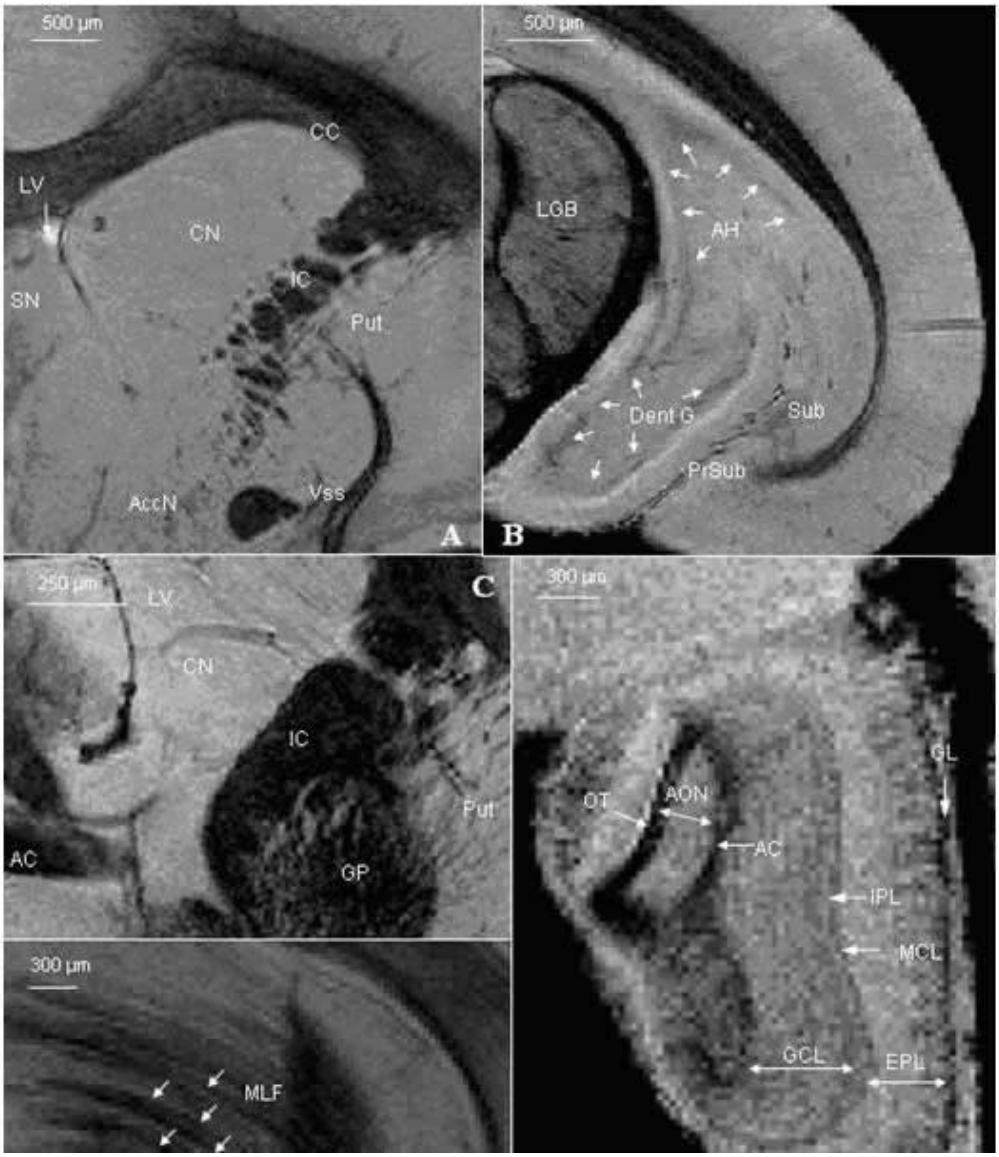

Ex vivo microscopic MRI of the mouse lemur brain after passive staining in a 2.5 mmol/L solution of Dotarem MR contrast agent (Guerbet, France). MRI acquisition was done on a 7T magnet using a 3D FLASH sequence with the following parameters: TR=200 ms, TE=20 ms, resolution: 31 µm x 31 µm x 120 µm. Abbreviations in A, B, C and D: AC: anterior commissure, AccN: accumbens nucleus, AH: Ammon's horn CC: corpus callosum, CN: caudate nucleus, Dent G: dentate gyrus, GB: globus pallidus, IC: internal capsule, LGB: lateral geniculate body, LV: lateral ventricle, MLF: medial lemniscus fibers, Put: putamen, SN: septal nuclei, Sub: subiculum, PreSub: Presubiculum, Vss: vessel. Abbreviations in E. AON: anterior olfactory nucleus, AC: anterior commissure, EPL: external plexiform layer, GCL: granule cell layer, GL: glomerular layer, IPL: internal plexiform layer, MCL: mitral cell layer, OT: olfactory tract.
IRM ex-vivo microscopique d'un cerveau de microcèbe après coloration dans 2.5 mmol/L d'une solution de Dotarem, un agent de contrast IRM (Guerbet, France). L'acquisition IRM a été effectuée à 7T avec une séquence 3D FLASH avec les paramètres suivants: TR=200 ms, TE=20 ms, resolution: 31 µm x 31 µm x 120 µm. Abréviations des encadrés A, B, C et D. AC: commissure antérieure, AccN: noyau accumbens, AH: corne d'Ammon, CC: corps calleux, CN: noyau caudé, Dent G: gyrus denté, GB: globus pallidus, IC: capsule interne, LGB: corps géniculé latéral, LV: ventricule latéral, MLF: fibre du lemnisque median, Put: putamen, SN: noyau septal, Sub: subiculum, PreSub: Presubiculum, Vss: vaisseaux sanguins. Abréviations de l'encadré E. AON: noyau olfactif antérieur, AC: commissure antérieure, EPL: couche plexiforme externe, GCL: couche des cellules granulaires, GL: couche glomérulaire, IPL: couche plexiforme interne, MCL: couche des cellules mitrales, OT: tractus olfactif.

4.2 Imaging the vascular system

14 MRI can be used to study the vascular anatomy in animals using angiography. This can be achieved using contrast agents but also without contrast agents. The latter method is of a particular interest for mouse lemurs as intravenous injections are particularly difficult in

these animals. Typical protocols to record angiograms in mouse lemurs are based on two dimensional gradient echo sequences (TR=30 ms, TE=3.9 ms, α=60°, FOV: 23x23 mm², slice thickness=0.4 mm, 85 slices overlapped by 0.2 mm, acquisition matrix: 192x192) and on the generation of maximum intensity projections (MIP) images which show the entire blood vessels. Example showing the vascular structure of mouse lemurs as compared to mice is presented in Fig. 4. In mouse models of Alzheimer's disease, alterations of angiograms have already been reported (El Tannir El Tayara *et al.*, 2010). These alterations can be evaluated in mouse lemurs thanks to MR angiograms.

Figure 4

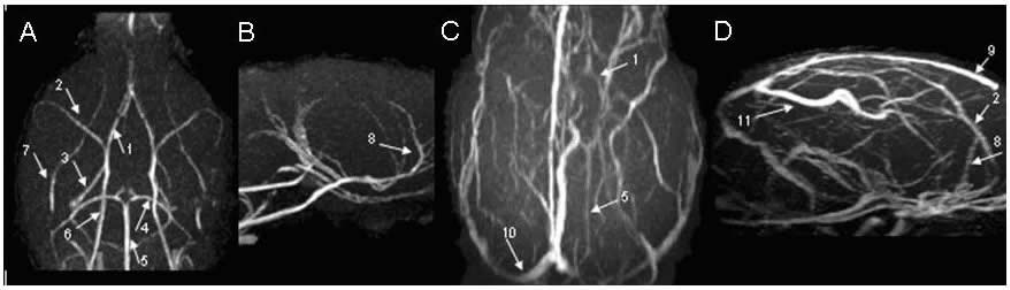

Comparison of the angiograms of a mouse (A: horizontal; B: sagittal views) and a mouse lemur (C: angiogram shifted by 24° with respect to the horizontal direction; D: sagittal view). Annotations: Arteries: 1. anterior, 2. middle, 3. posterior cerebral arteries, 4. superior cerebellar artery, 5. basilar artery, 6. internal carotid artery, 7. pterygopalatine artery, 8. azygos anterior cerebral artery; Veins: 9. superior sagittal sinus, 10. transverse sinus, 11. straight sinus.
Comparaison d'angiogrammes chez la souris (A: vue horizontale; B: vue sagittale) et chez un microcèbe (C: angiogramme pivoté de 24° dans le plan horizontal; D: vue sagittale). Annotations: Artères: 1. cérébrale antérieure, 2. cérébrale moyenne, 3. cérébrale postérieure, 4. cérébelleuse supérieure, 5. basilaire, 6. carotide interne, 7. ptérygopalatine, 8. cérébrale antérieure azygos; Veines: 9. sinus sagittal supérieur, 10. sinus transverse, 11. sinus droit.

5 Detection of age-associated cerebral changes in lemurs

5.1 Age-associated morphological alterations

Thanks to MR images, sporadic alterations can be detected in some animals (Fig. 5). For example, stroke (Fig. 5A-B) or compression of brain tissues due to extracranial mass can be detected in some animals (Fig. 5D).

Figure 5

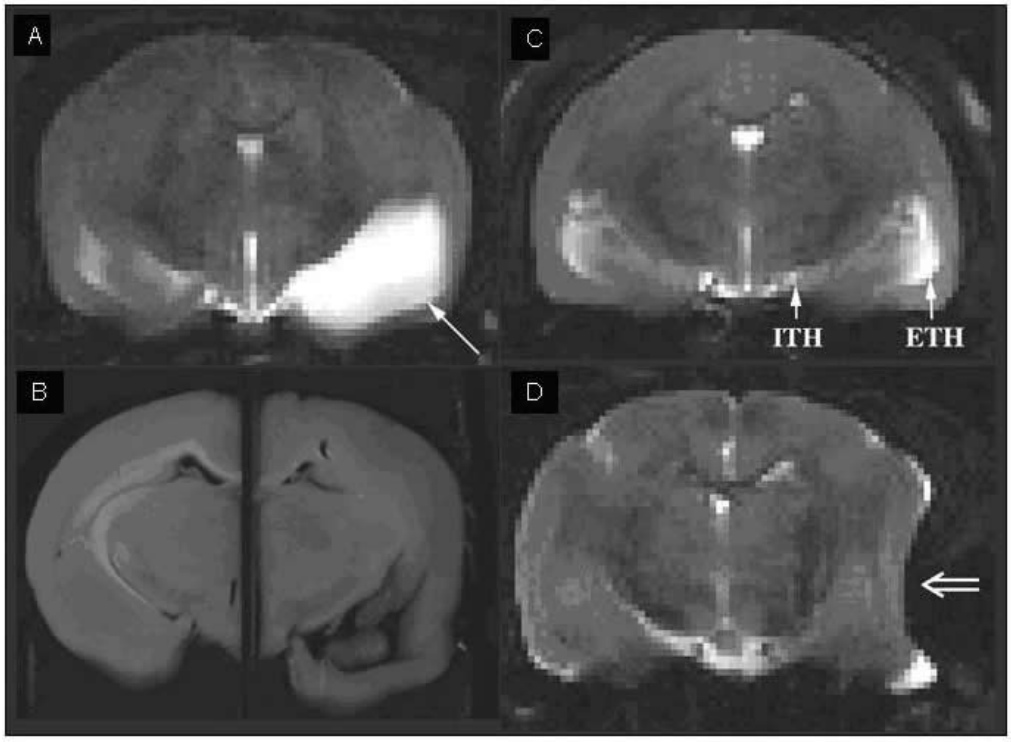

Detection of sporadic cerebral alterations in the brain of aged mouse lemurs. MRI (A, arrow) and neuropathological (non-stained section of a 1mm slice of the brain, B) detection of a severe unilateral dilatation of the left temporal horn of the lateral ventricle probably related to a vascular infarct in a mouse lemur. C. Dilatation of the external part of the temporal horn of the lateral ventricle (ETH). D. Compression of the left temporal area by an extra-axial expansive process, probably related to a former subdural abscess, hematoma, or meningioma in an aged mouse lemur. Other abbreviations. ITH: Internal part of the temporal horn of the lateral ventricle.
Détection d'altérations cérébrales sporadiques chez le microcèbe âgé. Détection IRM (A, flèche) et neuropathologique (tranche de cerveau de 1mm, non colorée, B) d'une dilatation unilatérale sévère de la corne temporale du ventricule latéral gauche, probablement liée à un infarctus cérébral chez le microcèbe. C. Dilatation du bord externe de la corne temporale du ventricule latéral (ETH). D. Compression de l'aire temporale gauche par un processus d'expansion extra-axial, probablement lié à un abcès subdural, un hématome ou un méningiome chez le microcèbe âgé. Autres abréviations. ITH: partie interne de la corne temporale du ventricule latéral.

16 In humans, during normal aging, cerebral atrophy is one of the most widely described cerebral alteration (Dekaban et Sadowsky, 1978; Good *et al.*, 2001). This alteration is particularly obvious during pathological aging, such as in the case of Alzheimer's disease (Valk *et al.*, 2002). The location and rate of atrophy depend on underlying pathological processes (Tisserand *et al.*, 2004). For example, during Alzheimer's disease the atrophy starts in temporal areas and progressively reaches all the brain regions (Baron *et al.*, 2001). In fronto-temporal dementia, the atrophy is more prominent in the frontal lobes and anterior temporal regions (Bocti *et al.*, 2006). In mouse models of Alzheimer's disease, cerebral atrophy is not obvious (Delatour *et al.*, 2006a). In contrast, cerebral atrophy has been largely described in mouse lemur primates using MRI assessment. The first MR study that evaluated atrophy in lemurs focused on the temporo-parietal area. It described in a series of 30 lemurs an atrophy process starting at an age between 5 and 8 years and evolving rapidly once initiated (Dhenain *et al.*, 2000). However, all the aged animals were not atrophied. Atrophy thus appears to be an age-related pathological condition and not an inevitable effect of age. A second study highlighted that this atrophy process shows regional specificity (Dhenain *et al.*, 2003). A third study demonstrated the existence of different patterns of atrophy, i.e. focal, multi-focal and generalized patterns. Indeed the atrophy pattern in lemurs leads to accumulation of cerebro-spinal fluid (CSF) first in the frontal pericortical areas, then in parietal and temporal regions and finally in all the pericortical regions. These patterns were consistent with a

progression of the atrophy starting from sharply demarcated regions toward a more generalized process encompassing the whole brain. Interestingly, a comparison of atrophy patterns and histology showed that atrophied animals have severe intracellular amyloid depositions as well as astrogliosis (Kraska *et al.*, 2010). The *in vivo* detection and follow-up of the atrophy process using MRI offers the possibility to search for the biological origin of ongoing neurodegeneration.

Figure 6

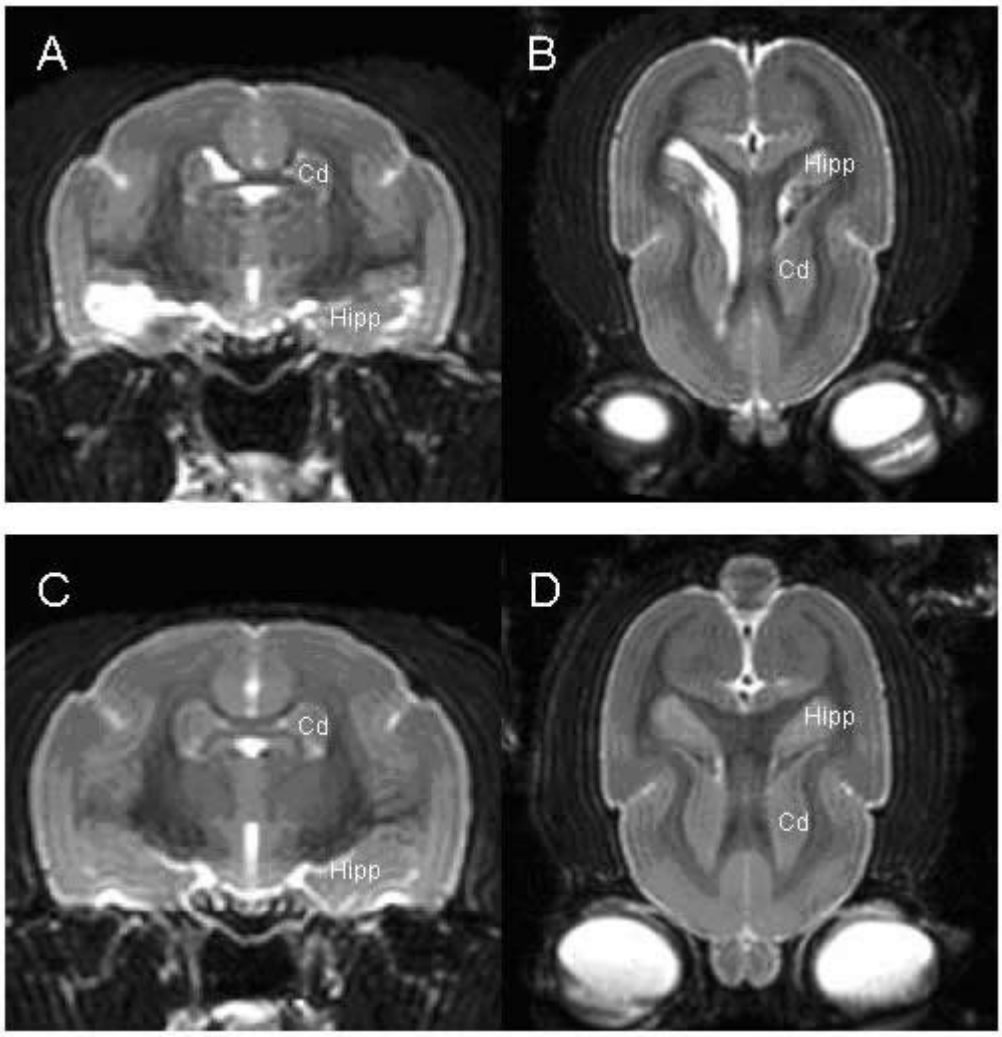

Typical profiles of cerebral atrophy in lemurs. A-B. Atrophied animal with CSF accumulation near hippocampus (Hipp) and caudate nucleus (Cd). C-D. In comparison, profile of an animal without any atrophic process. *In vivo* MRI acquisition was done on a 7T magnet using a T2-weighted sequence with the following parameters: TR=2500 ms, TE=69.2 ms, resolution=234 µm x 234 µm x 234 µm.
Profil d'atrophie cérébrale caractéristique chez le microcèbe. A-B. Animal atrophié avec une accumulation de liquide céphalo-rachidien près de l'hippocampe (Hipp) et du noyau caudé (Cd). C-D. Profil d'un animal sans aucun processus d'atrophie cérébrale. L'acquisition IRM in vivo a été faite à 7T avec une séquence pondérée en T2 avec les paramètres suivants : TR=2500 ms, TE=69.2 ms, résolution=234 µm x 234 µm x 234 µm.

5.2 Microhemorrhages

17 In humans, multi-infarct dementia is a major cause for age-related cognitive impairment (Fratiglioni *et al.*, 1999). In animals such as dogs (Bagley, 1997; Borras *et al.*, 1999) or monkeys (Prusty *et al.*, 1988; Uno, 1994), spontaneously occurring multiple infarctions are rarely described. However, the biochemical composition of cerebral vasculature changes with age (Sobin *et al.*, 1992). MRI is particularly sensitive to the detection of hemorrhages and such lesions lead to hypointense spots on MR images. As an example, the figure 7A shows the

detection of an artificially induced hemorrhage in a rat brain. The figure 7B displays patterns of microhemorrhages in aged mouse lemurs. These data suggest that vascular alterations are part of the alterations associated to cerebral aging in lemurs.

Figure 7

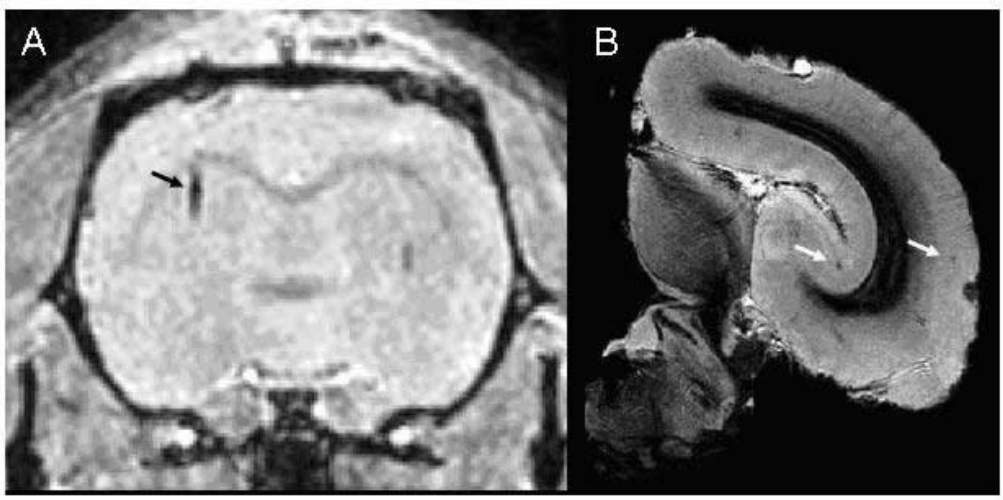

(A) Example showing detection by MRI of a hypointense lesions (arrow) corresponding to a hemorrhage in a rat brain. (B) displays patterns of microhemorrhages (arrows, hypointense spots) in aged mouse lemurs.
(A) Exemple montrant une détection IRM de lésions hypointenses (flèches) correspondant à des hémorragies cérébrales chez le rat. (B) Lésions semblables reflettant des microhémorragies (flèches, spots hypointenses) chez le microcèbe âgé.

5.3 Iron accumulation in the brain

18 In humans, during the first 30–35 years of life, iron accumulates in specific regions of the brain and then iron concentration reaches a plateau. The regions that are particularly involved in such accumulations are the globus pallidus and the substantia nigra. Other regions such as the red nucleus, the putamen, the caudate nucleus, the dentate nucleus as well as the subthalamic body also show large iron load (Hallgren et Sourander, 1958). Abnormal accumulation of iron has been reported in particular during the course of neurodegenerative diseases such as Parkinson's or Alzheimer's diseases (Zecca *et al.*, 2004).

19 MRI is also particularly sensitive to the detection of iron. Indeed, because of iron's paramagnetic characteristic, brain regions with high iron content have short T2 relaxation times yielding to a hypointense (dark) signal in T2-w or T2*-w images as compared to region with low iron content (Drayer, 1989). MRI analyses in humans have shown a rapid T2 signal decrease in young individuals, less rapid in middle-aged and slower in aged individuals (Pujol *et al.*, 1992; Schenker *et al.*, 1993; Bartzokis *et al.*, 1997). Stronger signals in key regions involved in AD or PD have also been observed, thus confirming histological results concerning the modulation of iron by aging and neurodegenerative diseases (Drayer *et al.*, 1986).

20 In mouse lemurs, MRI was the first method to highlight an age-related iron accumulation in the brain (Dhenain *et al.*, 1998)(Fig. 8). More specifically, iron accumulates in the globus pallidus, substantia nigra, neocortical and cerebellar white matter, thalamus, and in anterior forebrain structures, including the nucleus basalis of Meynert (Dhenain *et al.*, 1997a; Dhenain *et al.*, 1998; Gilissen *et al.*, 1998). In the basal forebrain, the areas of iron accumulation largely overlap the distribution of choline acetyltransferase (ChAT)-immunoreactive neurons (Gilissen *et al.*, 1999). However, unlike in humans, the signal decrease is continuous over the whole life span of the mouse lemur (Dhenain *et al.*, 1997a; Dhenain *et al.*, 1997b). Also very high correlations can be observed between the T2-w magnetic resonance imaging signal decrease and the natural logarithm of mouse lemur age in the pallidum, the substantia nigra, and in the thalamus (Dhenain *et al.*, 1997b). The T2 signal decreases rapidly until the age of

4 years. After this age, in middle-aged and older animals the signal decrease becomes less important.

Figure 8

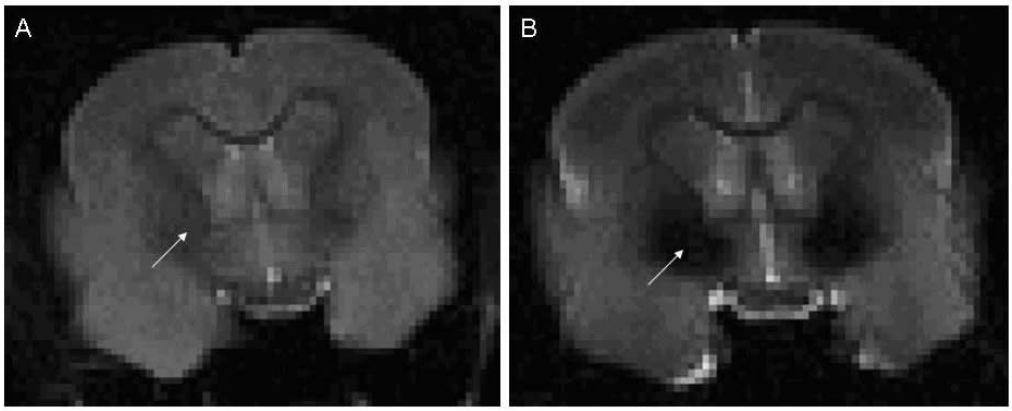

T2-w images from a young (A) and an old mouse lemurs (B) showing a reduced signal at the level of the globus pallidus (arrow) in the old animal. This signal decrease in the old animal is caused by iron accumulation in this brain region.
Images pondérées en T2 de microcèbes, jeune (A) et âgé (B), montrant un signal réduit au niveau du globus pallidus (flèche) chez l'animal âgé. La diminution de signal chez les vieux animaux est due à une accumulation de fer dans ces régions cérébrales.

6 Other applications of MRI in lemurs

6.1 Use of MRI during stereotaxic brain surgery in lemurs

21 Many models of neurodegenerative diseases are based on intracerebral injections of toxins and/or various drugs. In rats or mice, such injections rely on dedicated atlases that are used to calculate injection points relative to reference points such as the bregma. This region located on the top of the skull is the junction of the sagittal and coronal sutures. In the mouse lemur, a stereotaxic atlas has been published (Bons *et al.*, 1998). However the bregma position is changing as compared to the position of the brain (Fig. 9). Thus, the bregma can not be used as a reference as it is the case in rodents. In our laboratory, we implemented a method based on MRI to inject drugs in the brain of mouse lemurs. The method consists in sticking two capillaries filled with distilled water on the skull of mouse lemurs. One capillary is stuck on the bregma and another one is stuck parallel to the sagittal suture (Fig. 9G). A third visual cue (capillary) is placed to the right of the animal to know the position of the left and the right on the MR images. The animal is then placed into the scanner and MR images allow to visualize the location of the tubes. The targeted regions are localized on the images and the injection point (as compared to the capillaries) can be calculated (Anatomist software - http://brainvisa.info/index.html).

Figure 9

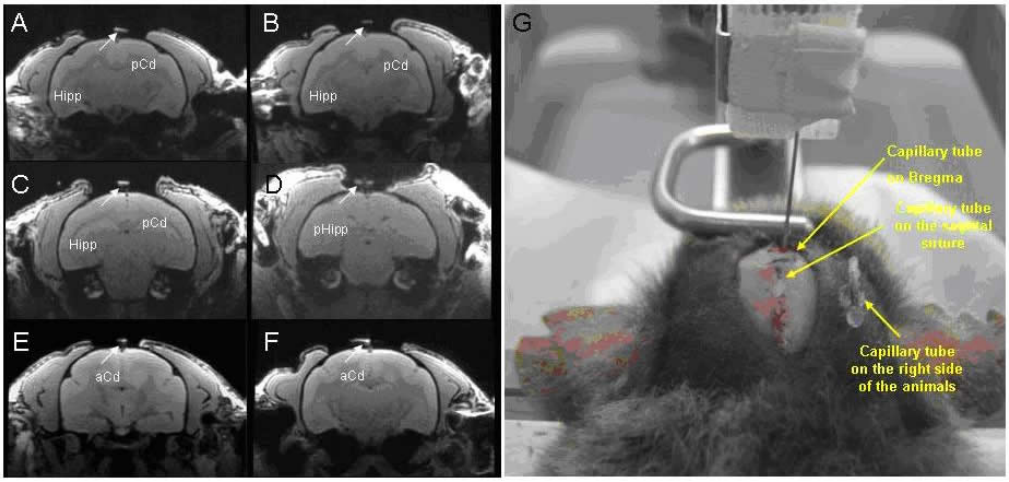

A-F. MRI showing capillary tubes (arrows) stuck at the level of the bregma on the skull of six mouse lemurs. One can see that the anatomical level varied greatly from one animal to the other. In A-C, the bregma was at the level of the hippocampus (Hipp) and posterior part of the caudate nucleus (pCd). In D, the bregma was at the level of the posterior part of the hippocampus (pHipp). In E-F, the bregma was at the level of the anterior part of the caudate nucleus (aCd). G. Mouse lemur in a stereotaxic frame. Capillary tubes are positioned at the level of the bregma, sagittal suture, and on the right side of the animal.

A-F. IRM montrant des tubes capillaires (flèches) fixés au niveau du bregma, sur le crâne de six microcèbes. On peut voir que le repère anatomique varie beaucoup d'un animal à l'autre. En A-C, le bregma était au niveau de l'hippocampe (Hipp) et de la partie postérieure du noyau caudé (pCd). En D, le bregma est situé au niveau de la partie postérieure de l'hippocampe (pHipp). En E-F, le bregma est au niveau de la partie antérieure du noyau caudé (aCd). G. Photo d'un microcèbe installé dans un cadre stéréotaxique. Les tubes capillaires sont positionnés au niveau du bregma, au niveau de la suture médiane et sur le côté droit de l'animal.

6.2 Use of MRI as a support to other imaging modalities

22 Other imaging modalities can be used to follow-up cerebral aging in mouse lemurs. Positron emission tomography is one of these modalities. This method is based on the injection of radioligands such as the 2-[18]-fluoro-2-deoxy-D-glucose (FDG). It allows to detect local metabolism in the brain of mouse lemurs. The resolution of PET images (0.47x0.47x0.80 mm^3) is not as fine as that of MR images and the contrast in the PET images is limited. These conditions do not allow to detect clearly anatomical regions (Fig. 10). MR images thus have to be registered on PET images in order to localize regions of interest (Fig. 10). This allows for a fine discrimination of the regions of interest in which the radioligand uptake is measured. The MR images co-registration on PET images can be performed with dedicated software such as for example Anatomist (http://brainvisa.info/index.html). MR and PET images are recorded for each animal and rigidly co-registered. The co-registration can be performed automatically or manually. The co-registration accuracy is checked thanks to benchmarks like eyes, olfactory bulbs, cerebellum, spinal cord and temporal lobes (Fig. 10).

Figure 10

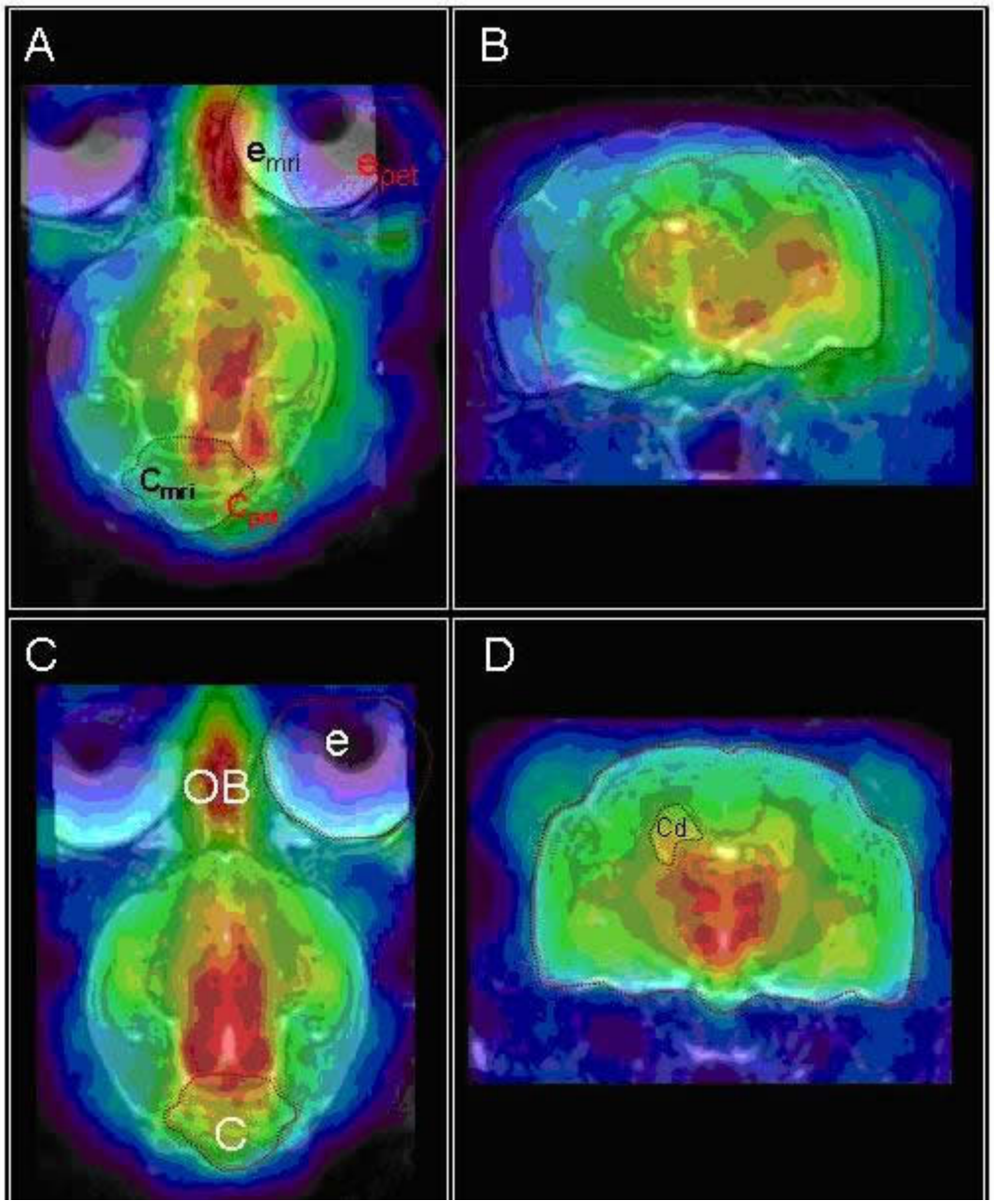

Use of MRI to identify anatomical structures on PET images thanks to PET and MR images co-registration. MR and PET images on A-B are not registered. PET images are the colored images, while the MR images are the images with anatomical details. In A, the shapes of the eye (e) and of the cerebellum (c) are outlined on the MR (black doted lines) and PET images (red doted lines). In B, the shape of the whole brain is outlined on the MR (black doted lines) and PET images (red doted lines). C-D show registered images. In D, the caudate nucleus (Cd) was outlined. The region of interest outlined in MR images can be used to evaluate the metabolism from the registered PET images. Other annotations: OB: olfactory bulb.

Utilisation de l'IRM pour identifier des structures anatomiques d'images en tomographie par émission de positons (TEP) grâce à un recalage entre les images TEP et IRM. A-B. Les images TEP et IRM ne sont pas mises en registre. Les images TEP sont les images en fausses couleurs et les images IRM sont les images avec des détails anatomiques. En A, la forme des yeux (e) et du cervelet (c) sont définies sur les images IRM (contour en pointillé noir) et sur les images TEP (contour en pointillé rouge). En B, la forme du cerveau entier est délimitée sur les images IRM (contour pointillé noir) et sur les images TEP (contour pointillé rouge). C-D montrent les images mises en registre. En D, le noyau caudé (Cd) a été délimité. Les régions d'intérêt définies sur les images IRM peuvent être utilisées pour évaluer le métabolisme régional sur les images TEP recalées. Autres annotations : OB : bulbe olfactif.

6.3 Towards evaluation of therapies in lemurs

23 Mouse lemurs are now more and more widely used to evaluate therapeutic interventions against aging and age-associated neurodegenerative diseases. For example, they are used to evaluate the effect of immunotherapies against Alzheimer's disease (Trouche *et al.*, 2009),

to evaluate caloric restriction or compounds such as resveratrol mimicking caloric restriction (Dal-Pan *et al.*, 2010) . Two difficulties are associated to the evaluation of therapies in lemurs. The first one is related to the heterogeneity of aging phenomena in lemurs. For example, cerebral atrophy involves only approximately 50% of the animals at the age of 5 years, with in addition various levels of atrophy for the animals. MRI can be used to select the animals with a given atrophy level in order to incorporate them in a therapeutic evaluation. The second one is related to the follow-up of animals during therapeutic evaluation. For example, Figure 11 shows the longitudinal follow-up of two mouse lemurs during immunotherapy treatment. In this study, animals were scanned before vaccination, and two, six and nine months after the beginning of the treatment. The *in vivo* MRI follow-up allows for the detection of not only a basal heterogeneity, but also visible cerebral changes in some cases (Fig. 11).

Figure 11

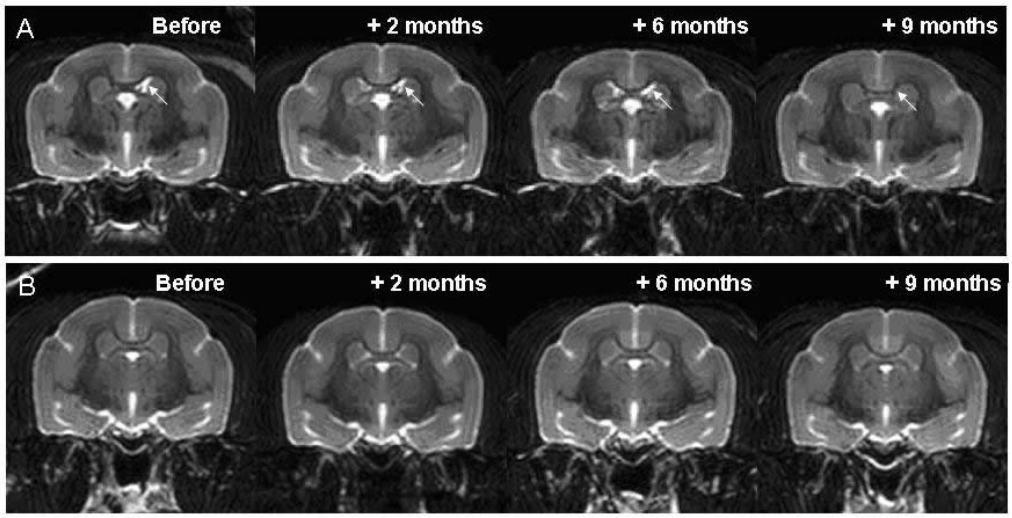

Follow-up of two mouse lemurs by MRI before and during immunotherapy. In the first case (A) the mouse lemur presented visible modulation of CSF pattern (arrow). In the second case (B) there was no visible modification of CSF level in the brain. The same sequence was used for the two animals and for all the sessions (for parameters see Fig. 6 legend).

Suivi IRM de deux microcèbes avant et pendant un traitement par immunothérapie. Dans le premier cas (A), le microcèbe présente une modulation de la quantité de LCR (flèche). Dans le second cas (B), aucune modification du LCR n'est détectée. La même séquence IRM a été utilisée pour les deux animaux lors de toutes les sessions (pour les paramètres voir Fig. 6).

7 Conclusion

24 Mouse lemurs are now used as relevant models of cerebral aging and age-associated neurodegenerative diseases. Because of their small size, they can be studied with widely available preclinical MR spectrometers. Many MRI studies can thus be performed in lemursto evaluate the brain in normal and pathological conditions. First, *in vivo* MRI and *ex vivo* MR histology allow for the accurate description of cerebral anatomy and the precise identification of structures of interest. Thus, MRI improves our knowledge of the anatomy of the mouse lemur brain. MRI is also a helpful tool when performing stereotaxic surgery in lemurs. Second, imaging methods allow for the characterization and the follow-up of cerebral aging biomarkers such as atrophic process, iron accumulation, microhemorrhages and cerebral glucose uptake. Third, *in vivo* MRI is a useful method to perform longitudinal study of therapeutic interventions. In our study of immunotherapy, the use of MRI leads to overcome the difficulties caused by the basal heterogeneity of aging biomarkers like atrophy.

25 MRI is thus an essential tool in any study evaluating cerebral aging in lemurs as it allows to detect and follow-up neurodegenerative alterations. In addition, the MRI methods used in mouse lemurs can be extended to other primate models of neurodegenerative diseases.

Bibliographie

Andersen AH, Zhang Z, Barber T, Rayens WS, Zhang J, Grondin R, Hardy P, Gerhardt GA, Gash DM (2002). Functional mri studies in awake Rhesus monkeys: Methodological and analytical strategies. *Journal Neurosci Meth* 118, 141-152.

Andersen AH, Zhang ZM, Zhang M, Gash DM, Avison MJ (1999). Age-associated changes in Rhesus cns composition identified by mri. *Brain Res* 829, 90-98.

Aujard F, Dhkissi-Benyahya O, Fournier I, Claustrat B, Schilling A, Cooper HM, Perret M (2001). Artificially accelerated aging by shortened photoperiod alters early gene expression (fos) in the suprachiasmatic nucleus and sulfatoxymelatonin excretion in a primate. *Neuroscience* 105, 403-412.

Bagley RS (1997). Common neurologic diseases of older animals. *Vet Clin North Am Small Anim Pract* 27, 1451-1486.

Baron JC, Chetelat G, Desgranges B, Perchey G, Landeau B, de la Sayette V, Eustache F (2001). In vivo mapping of gray matter loss with voxel-based morphometry in mild Alzheimer's disease. *Neuroimage* 14, 298-309.

Bartus RT, Dean RL (1985). Developing and utilizing animal models in the search for an effective treatment for age-related memory disturbances. In *Normal aging, Alzheimer's disease and senile dementia: Aspects on etiology, pathogenesis, diagnosis and treatment* (Gottfries CG, editor). Brussels: Éditions de l'Université de Bruxelles. pp 231-265.

Bartzokis G, Beckson M, Hance DB, Marx P, Foster JA, Marder SR (1997). MR evaluation of age-related increase of brain iron in young adult and older normal males. *Magn Reson Imaging* 15, 29-35.

Bocti C, Rockel C, Roy P, Gao F, Black SE (2006). Topographical patterns of lobar atrophy in frontotemporal dementia and Alzheimer's disease. *Dement Geriatr Cogn* 21, 364-372.

Bons N, Jallageas V, Silhol S, Mestre-Frances N, Petter A, Delacourte A (1995). Immunocytochemical characterization of tau proteins during cerebral aging of the lemurian primate microcebus murinus. *C R Acad Sci III* 318, 77-83.

Bons N, Mestre N, Petter A (1991). Senile plaques and neurofibrillary changes in the brain of an aged lemurian primate, *Microcebus murinus*. *Neurobiol Aging* 13, 99-105.

Bons N, Sihol S, Barbier V, Mestre-Frances N, Albe-Fessard D (1998). A stereotaxic atlas of the grey lesser mouse lemur brain (*Microcebus murinus*). *Brain Res Bull* 46, 1-173.

Borras D, Ferrer I, Pumarola M (1999). Age-related changes in the brain of the dog. *Vet Pathol* 36, 202-211.

Carmichael ST (2005). Rodent models of focal stroke: Size, mechanism, and purpose. *NeuroRx* 2, 396-409.

Crook T, Bartus RT, Ferris SH, Whitehouse P, Cohen GD, Gershon S (1986). Age-associated memory impairment: Proposed diagnostic criteria and measures of clinical change: Report of a nimh work group. *Dev Neuropsychol* 2, 261-276.

Dal-Pan A, Terrien J, Pifferi F, Botalla R, Hardy I, Marchal J, Zahariev A, Chery I, Zizzari P, Perret M, Picq JL, Epelbaum J, Blanc S, Aujard F (2010 - doi 10.1007/s11357-010-9156-6). Caloric restriction or resveratrol supplementation and ageing in a non-human primate: First-year outcome of the restrikal study in *Microcebus murinus*. *Age (Dordr)*.

Dekaban AS, Sadowsky D (1978). Changes in brain weights during the span of human life: Relation of brain weights to body heights and body weights. *Ann Neurol* 4, 345-356.

Delacourte A, Sautière P-E, Wattez A, Mourton-Gilles C, Petter A, Bons N (1995). Biochemical characterisation of tau proteins during cerebral aging of the lemurian primate *Microcebus murinus*. *C R Acad Sci III* 318, 85-89.

Delatour B, Guegan M, Volk A, Dhenain M (2006a). In vivo mri and histological evaluation of brain atrophy in app/ps1 transgenic mice. *Neurobiol Aging* 27, 835-847.

Delatour B, Le Cudennec C, El Tannir-El Tayara N, Dhenain M (2006b). Transgenic models of Alzheimer's pathology: Success and caveat. In *Topics in Alzheimer's disease* (Welsh EM, editor). Nova Publishers. pp 1-34.

Dhenain M, Chenu E, Hisley CK, Aujard F, Volk A (2003). Regional atrophy in the brain of lissencephalic mouse lemur primates: Measurement by automatic histogram-based segmentation of mr images. *Magn Reson Med* 50, 984-992.

Dhenain M, Delatour B, Walczak C, Volk A (2006). Passive staining: A novel ex vivo mri protocol to detect amyloid deposits in mouse models of Alzheimer's disease. *Magn Reson Med* 55, 687-693.

Dhenain M, Duyckaerts C, Michot J-L, Volk A, Picq J-L, Boller F (1998). Cerebral t2-weighted signal decrease during aging in the mouse lemur primate reflects iron accumulation. *Neurobiol Aging* 19, 65-69.

Dhenain M, Michot J-L, Volk A, Picq J-L, Boller F (1997a). T2-weighted mri studies of mouse lemurs: A primate model of brain aging. *Neurobiol Aging* 18, 517-521.

Dhenain M, Michot JL, Privat N, Picq JL, Boller F, Duyckaerts C, Volk A (2000). Mri description of cerebral atrophy in mouse lemur primates. *Neurobiol Aging* 21, 81-88.

Dhenain M, Volk A, Picq J-L, Perret M, Boller F, Michot J-L (1997b). Age dependence of the t2-weighted mri signal in brain structures of a prosimian primate (*Microcebus murinus*). *Neurosci Lett* 237, 85-88.

Drayer B, Burger P, Darwin R, Riederer S, Herfkens R, Johnson GA (1986). Magnetic resonance imaging of brain iron. *Am J Neuroradiol* 7, 373-380.

Drayer BP (1989). Basal ganglia: Significance of signal hypointensity on t2-weighted mr images. *Radiology* 173, 311-312.

El Tannir El Tayara N, Delatour B, Volk A, Dhenain M (2010 - doi 10.1007/s10334-009-0194-y). Detection of vascular alterations by in vivo magnetic resonance angiography and histology in app/ps1 mouse model of Alzheimer's disease. *MAGMA* 23, 53-64.

Faure A, Verret L, Bozon B, El Tannir El Tayara N, Ly M, Kober F, Dhenain M, Rampon C, Delatour B (2009 - doi:10.1016/j.neurobiolaging.2009.03.009). Impaired neurogenesis, neuronal loss, and brain functional deficits in the appxps1-ki mouse model of Alzheimer's disease. *Neurobiol Aging*.

Fratiglioni L, De Ronchi D, Aguero-Torres H (1999). Worldwide prevalence and incidence of dementia. *Drug Aging* 15, 365-375.

Fratiglioni L, Launer LJ, Andersen K, Breteler MM, Copeland JR, Dartigues JF, Lobo A, Martinez-Lage J, Soininen H, Hofman A (2000). Incidence of dementia and major subtypes in europe: A collaborative study of population-based cohorts. Neurologic diseases in the elderly research group. *Neurology* 54, S10-15.

Fukuda S, del Zoppo GJ (2003). Models of focal cerebral ischemia in the nonhuman primate. *ILAR J* 44, 96-104.

Gilissen EP, Ghosh P, Jacobs RE, Allman JM (1998). Topographical localization of iron in brains of the aged fat-tailed dwarf lemur (*Cheirogaleus medius*) and gray lesser mouse lemur (*Microcebus murinus*). *Am J Primatol* 45, 291-299.

Gilissen EP, Jacobs RE, Allman JM (1999). Magnetic resonance microscopy of iron in the basal forebrain cholinergic structures of the aged mouse lemur. *J Neurol Sci* 168, 21-27.

Good CD, Johnsrude IS, Ashburner J, Henson RN, Friston KJ, Frackowiak RS (2001). A voxel-based morphometric study of ageing in 465 normal adult human brains. *Neuroimage* 14, 21-36.

Hallgren B, Sourander P (1958). The effect of age on the non-haemin iron in the human brain. *J Neurochem* 3, 41-55.

Harvey BK, Wang Y, Hoffer BJ (2008). Transgenic rodent models of parkinson's disease. *Acta Neurochir Suppl* 101, 89-92.

Jarraya B, Boulet S, Ralph GS, Jan C, Bonvento G, Azzouz M, Miskin JE, Shin M, Delzescaux T, Drouot X, Herard AS, Day DM, Brouillet E, Kingsman SM, Hantraye P, Mitrophanous KA, Mazarakis ND, Palfi S (2009). Dopamine gene therapy for parkinson's disease in a nonhuman primate without associated dyskinesia. *Sci Transl Med* 1, 2ra4.

Kappeler C, Dhenain M, Phan Dinh Tuy F, Saillour Y, Marty S, Fallet-Bianco C, Souville I, Souil E, Pinard J-M, Meyer G, Encha-Razavi F, Volk A, Beldjord C, Chelly J, Francis F (2007). Mri and histological studies of corpus callosal and hippocampal abnormalities linked to doublecortin deficiency. *J Comp Neurol* 500, 239-254.

Koo BB, Schettler SP, Murray DE, Lee JM, Killiany RJ, Rosene DL, Kim DS, Ronen I (2010 - doi 10.1016/j.neurobiolaging.2010.07.010). Age-related effects on cortical thickness patterns of the Rhesus monkey brain. *Neurobiol Aging*.

Kraska A, Dorieux O, Picq J-L, Petit F, Bourrin E, Chenu E, Volk A, Perret M, Hantraye P, Mestre-Frances N, Aujard F, Dhenain M (2010 - doi 10.1016/j.neurobiolaging.2009.05.018). Age associated cerebral atrophy in mouse lemur primates. *Neurobiol Aging*.

Lacreuse A, Diehl MM, Goh MY, Hall MJ, Volk AM, Chhabra RK, Herndon JG (2005). Sex differences in age-related motor slowing in the Rhesus monkey: Behavioral and neuroimaging data. *Neurobiol Aging* 26, 543-551.

Lacreuse A, Herndon JG (2009). Nonhuman primate models of cognitive aging In *Animal models of human cognitive aging* New-York: Humana Press. pp 1-30.

Lauterbur PC (1973). Image formation by induced local interactions. Examples employing nuclear magnetic resonance. *Nature*, 190-191.

Le Gros Clark WE (1931). The brain of *microcebus murinus*. *Proceedings of the Zoological Society of London*, 463-485.

Leite FP, Tsao D, Vanduffel W, Fize D, Sasaki Y, Wald LL, Dale AM, Kwong KK, Orban GA, Rosen BR, Tootell RB, Mandeville JB (2002). Repeated fmri using iron oxide contrast agent in awake, behaving macaques at 3 tesla. *Neuroimage* 16, 283-294.

Makris N, Kennedy DN, Boriel DL, Rosene DL (2010). Methods of mri-based structural imaging in the aging monkey. *Methods* 50, 166-177.

Mansfield P, Grannell PK (1973). Nmr `diffraction' in solids? *J Phys C: Solid State Phys* 6, L422.

Mestre-Frances N, Keller E, Calenda A, Barelli H, Checler F, Bons N (2000). Immunohistochemical analysis of cerebral cortical and vascular lesions in the primate *Microcebus murinus* reveal distinct amyloid beta 1-42 and beta 1-40 immunoreactivity profiles. *Neurobiol Dis* 7, 1-8.

Oikawa N, Kimura N, Yanagisawa K (2010). Alzheimer-type tau pathology in advanced aged nonhuman primate brains harboring substantial amyloid deposition. *Brain Res* 1315, 137-149.

Perret M (1997). Change in photoperiodic cycle affects life span in a prosimian primate (*Microcebus murinus*). *J Biol Rhythm* 12, 136-145.

Picq J-L, Aujard F, Volk A, Dhenain M (2010 - doi:10.1016/j.neurobiolaging.2010.09.009). Age-related cerebral atrophy in non-human primates predicts cognitive impairments. *Neurobiol Aging*.

Price DL, Martin LJ, Sisodia SS, Wagster MV, Koo EH, Walker LC, Koliatsos VE, Cork LC (1991). Aged non-human primates: An animal model of age-associated neurodegenerative disease. *Brain Pathol* 1, 287-296.

Prusty S, Kemper T, Moss MB, Hollander W (1988). Occurrence of stroke in a nonhuman primate model of cerebrovascular disease. *Stroke* 19, 84-90.

Pujol J, Junqué C, Vandrell P, M. Grau J, Marti-Vilalta JL, Olivé C, Gili J (1992). Biological significance of iron-related magnetic resonance imaging changes in the brain. *Arch Neurol-Chicago* 49, 711-717.

Rocca WA (2000). Dementia, parkinson's disease, and stroke in europe: A commentary. *Neurology* 54, S38-40.

Roth GS, Mattison JA, Ottinger MA, Chachich ME, Lane MA, Ingram DK (2004). Aging in Rhesus monkeys: Relevance to human health interventions. *Science* 305, 1423-1426.

Schenker C, Meier D, Wichmann W, Boesiger P, Valavanis A (1993). Age distribution and iron dependency of the t2 relaxation time in the globus pallidus and putamen. *Neuroradiology* 35, 119-124.

Shimada A, Ohta A, Akiguchi I, Takeda T (1992). Inbred sam-p/10 as a mouse model of spontaneous, inherited brain atrophy. *J Neuropath Exp Neur* 51, 440-450.

Smith DE, Rapp PR, McKay HM, Roberts JA, Tuszynski MH (2004). Memory impairment in aged primates is associated with focal death of cortical neurons and atrophy of subcortical neurons. *J Neurosci* 24, 4373-4381.

Sobin SS, Bernick S, Ballard KW (1992). Histochemical characterization of the aging microvasculature in the human and other mammalian and non-mammalian vertebrates by the periodic acid-schiff reaction. *Mech Ageing Dev* 63, 183-192.

Tigges J, Gordon TP, McClure HM, Hall EC, Peters A (1988). Survival rate and life span of Rhesus monkeys at the yerkes regional primate research center. *Am J Primatol* 15, 195-285.

Tisserand DJ, van Boxtel MP, Pruessner JC, Hofman P, Evans AC, Jolles J (2004). A voxel-based morphometric study to determine individual differences in gray matter density associated with age and cognitive change over time. *Cereb Cortex* 14, 966-973.

Trouche SG, Asuni A, Rouland S, Wisniewski T, Frangione B, Verdier JM, Sigurdsson EM, Mestre-Frances N (2009). Antibody response and plasma abeta1-40 levels in young *Microcebus murinus* primates immunized with abeta1-42 and its derivatives. *Vaccine* 27, 957-964.

Uno H (1994). The incidence of senile plaques and multiple infarction in aged macaque brain. *Neurobiol Aging* 14, 673-674.

Uno H, Alsum PB, Dong S, Richardson R, Zimbric ML, Thieme CS, Houser WD (1996). Cerebral amyloid angiopathy and plaques, and visceral amyloidosis in aged macaques. *Neurobiol Aging* 17, 275-281.

Valk J, Barkhof F, Scheltens P (2002). *Magnetic resonance in dementia*. Heidelberg Berlin New York: Springer-Verlag.

Yu X, Wang S, Chen DY, Dodd S, Goloshevsky A, Koretsky AP (2010). 3d mapping of somatotopic reorganization with small animal functional mri. *Neuroimage* 49, 1667-1676.

Zecca L, Youdim MB, Riederer P, Connor JR, Crichton RR (2004). Iron, brain ageing and neurodegenerative disorders. *Nat Rev Neurosci* 5, 863-873.

Notes

1 Acknowledgements: We thank N. Mestre-Frances, E. M. Sigurdsson, F. Aujard, and M. Perret for providing the animals and material used to record the images that illustrate this article. P. Hantraye is acknowledged for useful discussions. Our work on mouse lemurs was supported by the Aging ATC 2002 (INSERM), the Fédération pour la Recherche sur le Cerveau 2003, the ACI Neurosciences 2004 (French Research Department), the France-Alzheimer association, the longevity program from the CNRS, the National Foundation for Alzheimer's Disease and Related Disorders, and the National Institute on Aging (R01-AG020197). NJM is funded by the Martinique Region. AB is funded by the French Society of Radiology, the French Society of Neuroradiology, the French Ministry of Foreign Affairs (EGIDE funding) and the Philippe Foundation.

Pour citer cet article

Référence électronique
Nelly Joseph-Mathurin, Olene Dorieux, Audrey Kraska, Anne Bertrand, Mathieu Santin, Nadine El Tannir El Tayara et Marc Dhenain, « Magnetic resonance imaging in primates. The example of the mouse lemur (*Microcebus murinus*): From detection of pathological aging to therapeutic evaluations », *Revue de primatologie* [En ligne], 2 | 2010, document 5, mis en ligne le 15 juin 2011. URL : http://primatologie.revues.org/508

À propos des auteurs

Nelly Joseph-Mathurin
CEA, DSV, I2BM, MIRCen, CNRS, URA CEA CNRS 2210, 18 route du panorama 92265 Fontenay-aux-Roses cedex, France.
Olene Dorieux

CEA, DSV, I2BM, MIRCen, CNRS, URA CEA CNRS 2210, 18 route du panorama 92265 Fontenay-aux-Roses cedex, France, and CNRS UMR 7179, MNHN, 4 Avenue du Petit Château, 91800 Brunoy, France.

Audrey Kraska
CEA, DSV, I2BM, MIRCen, CNRS, URA CEA CNRS 2210, 18 route du panorama 92265 Fontenay-aux-Roses cedex, France, and Institut de Recherche SERVIER, 125 Chemin de Ronde, 78290 Croissy-sur-Seine, France.

Anne Bertrand
CEA, DSV, I2BM, MIRCen, CNRS, URA CEA CNRS 2210, 18 route du panorama 92265 Fontenay-aux-Roses cedex, France, and Department of Physiology and Neuroscience, Medical Science Building MSB 453, New York University School of Medicine, 550 First Avenue, New York, NY 10016, USA.

Mathieu Santin
CEA, DSV, I2BM, MIRCen, CNRS, URA CEA CNRS 2210, 18 route du panorama 92265 Fontenay-aux-Roses cedex, France, and Sanofi-Aventis, TSU Aging - Disablilities Heart & Brain, 1 avenue Pierre Brossolette 91385 Chilly-Mazarin cedex, France.

Nadine El Tannir El Tayara
Institut Curie, U759 INSERM, Centre Universitaire Labo 112, 91405, Orsay Cedex, France.

Marc Dhenain
CEA, DSV, I2BM, MIRCen, CNRS, URA CEA CNRS 2210, 18 route du panorama 92265 Fontenay-aux-Roses cedex, France, and CEA, DSV, I2BM, NeuroSpin, Centre CEA de Saclay, Bât. 145, 91191 Gif sur Yvette, France.
Author for correspondence: Marc.Dhenain@cea.fr

Abstract / Résumé

Cerebral aging is a major public health issue in our societies as the aged population increases dramatically. It leads in many cases to neurodegenerative diseases such as Alzheimer disease (AD). Rodents and particularly transgenic mice are widely used as models for research on physiopathology of cerebral aging, neurodegenerative diseases and for the evaluation of therapies. However these models do not mimic all the pathophysiological aspects of human diseases. Complementary models such as non-human primates are phylogenetically close to humans and thus more predictive of drug efficiency in humans. Mouse lemur (*Microcebus murinus*) is a small primate (about 12cm, 100g) described as a useful model of cerebral aging and as a potential model of AD. Indeed several animals develop age-associated cerebral alterations like amyloidosis and other cerebral changes. Non invasive medical imaging methods such as magnetic resonance imaging (MRI) can be used to follow-up brain changes in these animals. In this review, we present how mouse lemurs can be followed-up by MRI and how MRI can be used during therapeutic evaluations and other applications in this model. MR images can be used to follow-up cerebral anatomy in mouse lemurs. It allows for the description of age-associated atrophic processes, age-associated iron accumulation, and vascular anatomy (thanks to MR angiography). Cerebral glucose uptake can be studied in mouse lemurs with other *in vivo* imaging modalities such as positron emission tomography (PET). In this case, MRI can be used as a support for quantification of radioligand uptake in specific structures. *Ex vivo* MR imaging is another MR protocol that can be used to describe cerebral aging in lemurs. It provides high resolution 3D histological brain images and allows for studying exquisite anatomical details or microhemorrhages. Finally, MRI can be used to practice cerebral surgery in lemurs and determine coordinates for stereotactic injections. It can also be used during therapeutic interventions by selecting animals to be involved in therapeutic

trials and also by following specific MR biomarkers. MRI is thus critical to better characterize cerebral aging in the mouse lemur and to better carry out longitudinal studies in this primate model.

Imagerie par résonance magnétique chez les primates. L'exemple du microcèbe murin (*Microcebus murinus*) : De la détection du vieillissement cérébral pathologique à l'évaluation thérapeutique

Le vieillissement cérébral est un problème majeur de santé public. Il est associé dans certains cas à des maladies neurodégénératives telles que la maladie d'Alzheimer (MA). La compréhension de la physiopathologie du vieillissement cérébral et l'évaluation de nouvelles thérapies nécessitent l'utilisation de modèles animaux. Les souris transgéniques sont très utilisées mais restent peu représentatives de l'ensemble des aspects des maladies humaines. Les modèles primates sont plus proches phylogénétiquement de l'homme et sont plus prédictifs de l'efficacité de médicaments chez l'homme. Le microcèbe murin est un petit primate (environ 12cm, 100g) qui est un modèle de vieillissement cérébral et un modèle potentiel de la MA. En effet certains animaux développent avec l'âge des altérations cérébrales telles que de l'amyloïdose. Des méthodes d'imagerie non-invasives comme l'imagerie par résonance magnétique (IRM) peuvent être utilisées pour étudier les altérations cérébrales chez ces animaux. Nous montrons ici comment l'IRM permet d'étudier le microcèbe et présentons l'utilisation de l'IRM pour l'évaluation de thérapies et d'autres applications. Chez le microcèbe, l'IRM a permis de décrire l'anatomie cérébrale, le système vasculaire cérébral (grâce à l'angiographie par RMN) et aussi de caractériser l'atrophie cérébrale liée à l'âge ainsi que des processus entraînant une accumulation de fer intracérébrale. La consommation cérébrale de glucose a aussi pu être étudiée par une autre modalité d'imagerie *in vivo*, la tomographie par émission de positons (TEP). Dans ce cas, l'IRM sert de support pour quantifier la consommation du radioligand dans des structures spécifiques. De plus, en modalité *ex vivo*, l'IRM permet d'obtenir des images 3D histologiques de haute résolution et permet ainsi d'étudier des détails anatomiques très fins ou des microhémorragies. Enfin, l'IRM peut servir de support à des interventions chirurgicales comme lors d'injections intracérébrales pour lesquelles elle aide à déterminer les coordonnées stéréotaxiques. Elle peut également être utilisée pour le suivi d'interventions thérapeutiques car elle permet la sélection et le suivi des animaux participant à l'essai thérapeutique grâce à des biomarqueurs IRM. L'IRM est donc cruciale pour améliorer la caractérisation du vieillissement cérébral chez le microcèbe et pour améliorer la mise en œuvre d'études longitudinales chez ce modèle.

Mots clés : MRI, imaging, mouse lemur, primates, aging, Alzheimer, IRM, imagerie, microcèbe, primates, vieillissement, Alzheimer

Thématique : Méthodes